VIBRATORY SURFACE LOADINGS ON A VISCOELASTIC HALF-SPACE

T.M. Lee

September 1970

CONTRACT DAAG23-68-C-0018

DA TASK 1T025001A130-01

CORPS OF ENGINEERS, U.S. ARMY
COLD REGIONS RESEARCH AND ENGINEERING LABORATORY
HANOVER, NEW HAMPSHIRE

PREFACE

This report was prepared by Dr. T.M. Lee, School of Engineering, San Fernando Valley State College, Northridge, California, under Contract DAAG23-68-C-0018 with the U.S. Army Cold Regions Research and Engineering Laboratory, as part of DA Task 1T025001A130-01.

The work was conducted under the supervision of Mr. A.F. Wuori, Chief, Applied Research Branch and under the general direction of Mr. K.A. Linell, Chief, Experimental Engineering Division, USA CRREL.

The author wishes to express his appreciation to Mr. Wuori and Mr. Linell for their encouragement and support of his research. He is especially indebted to Mr. H.W. Stevens of USA CRREL whose unfailing effort and continuous cooperation made this project possible.

The report has been technically reviewed by Dr. Y. Nakano, Physical Sciences Branch, Research Division, USA CRREL.

CONTENTS

ILLUSTRATIONS

CONTENTS (Cont'd)

TABLES

VIBRATORY SURFACE LOADINGS ON A VISCOELASTIC HALF-SPACE

by

T.M. Lee

INTRODUCTION

It has been the usual practice[1] to apply the theory of linear elasticity when designing foundations involving vibratory loads. Experience has shown that the theory is normally adequate for design but is not always realistic. One reason is that it does not include the effect of internal damping of the soil. Internal damping is a property affecting the stress-strain relationship by introducing time dependence. Viscoelastic theory takes such time dependence into account. It is suggested that under low stress vibratory loads, many soils may reasonably be considered to behave like a viscoelastic material.

Wave propagation in an elastic half-space generated by an impulsive force applied at its surface was first considered by Lamb[3] in his classic paper *On the Propagation of Tremors Over the Surface of an Elastic Solid.* This study was later extended by Reissner[8] to consider the effect of a group of periodic surface forces uniformly distributed over a circular area. The same problem was treated by Sung[10] and Quinlan[7] for two more cases of loading distribution: namely, 1) parabolic distribution of the forces, and 2) forces to approximate the static reactions under a circular rigid plate. Sung also provides tables and curves in his paper that can be used to determine the elastic constants of a given foundation with appropriate tests. In considering machine foundation design, Hsieh[2] reworked the Reissner-Sung theory for evaluating the damping effect of its supporting medium. Since the original analysis[7,8,10] was based on *elastic* theory, the *damping* effect referred to is that due to geometric dispersion rather than the dissipative property of the medium.

To include the damping effect from energy dissipation, it is proposed to consider the ground as a viscoelastic medium and make an analysis based on the assumption that it is a homogeneous, isotropic, linear viscoelastic half-space.[6]

The work presented here is subdivided into two parts. Solutions to the displacement functions for a viscoelastic half-space subjected to surface loadings are presented in the first part. As will be shown, surface vibrations in areas near the source (near field) are affected by three types of waves generated by the source, namely dilatational waves, shear waves, and Rayleigh (surface) waves. The first two types of waves diminish with distance much more rapidly than the third kind. Hence, at *great* distances from the source (far field), only the effect of the Rayleigh waves needs to be considered. With this simplification, closed form expressions for surface motions at great distances are obtained in this portion of the analysis. A field method of using these results to determine the complex modulus and the damping property of a viscoelastic material[3,4] is proposed.

In the second part of this work, the near field effect of vibratory loadings over a surface circular area is examined and the vertical motion at the center of the circle is calculated for the three types of force distribution as used by Reissner and Sung. Under these loading conditions, the displacement function is found to depend on the frequency of the applied load and also on the properties

of the supporting medium. Using these as parameters, a fairly broad range of computations for the center displacements can be provided in table form. However, to facilitate the computation, an attempt has been made to reconstruct the center displacement as a *simple* function of the (load) vibration frequency and the material properties of the half-space. With these relationships, computations may be accomplished without using a computer; furthermore, computation time will be only a small fraction of that required for the original analysis.

BASIC ANALYSIS

The wave equation in a homogeneous, isotropic, linear viscoelastic medium may be expressed:[5]

$$[\lambda(i\omega) + 2\mu(i\omega)]\,\nabla^2\phi = \rho\,\frac{\partial^2\phi}{\partial t^2} \tag{1}$$

$$\mu(i\omega)\nabla^2\psi = \rho\,\frac{\partial^2\psi}{\partial t^2} \tag{2}$$

where ϕ and ψ are dilatational and shear potentials, respectively,

$$\lambda(i\omega) = \lambda'(\omega) + i\lambda''(\omega)$$

$$\mu(i\omega) = \mu'(\omega) + i\mu''(\omega)$$

are the complex Lame's constants, ρ is the density of the medium, and ∇^2 denotes the Laplacian operator.

Introducing

$$c_1^2(i\omega) = \frac{\lambda(i\omega) + 2\mu(i\omega)}{\rho}, \tag{3a}$$

$$c_2^2(i\omega) = \frac{\mu(i\omega)}{\rho}; \tag{3b}$$

eq 1 and 2 can be rewritten as

$$c_1^2(i\omega)\nabla^2\phi = \frac{\partial^2\phi}{\partial t^2} \tag{4}$$

$$c_2^2(i\omega)\nabla^2\psi = \frac{\partial^2\psi}{\partial t^2}. \tag{5}$$

Applying first the Fourier transform and then the Hankel transform[9] to eq 4 and 5, we get, after rearranging,

$$\frac{\partial^2\Phi(k,z,\omega)}{\partial z^2} - \left[k^2 - \frac{\omega^2}{c_1^2(i\omega)}\right]\Phi(k,z,\omega) = 0, \tag{6}$$

$$\frac{\partial^2 \Psi(k, z, \omega)}{\partial z^2} - \left[k^2 - \frac{\omega^2}{c_2^2(i\omega)} \right] \Psi(k, z, \omega) = 0. \tag{7}$$

The solutions of eq 6 and 7 may be written as:

$$\Phi(k, z, \omega) = A(k, \omega)\, e^{-qz}\, P(k, \omega) \tag{8}$$

$$\Psi(k, z, \omega) = B(k, \omega)\, e^{-sz}\, P(k, \omega) \tag{9}$$

where $A(k, \omega)$ and $B(k, \omega)$ are to be determined from the boundary conditions of the problem, $P(k, \omega)$ is the transformed load function,

$$q^2(k, \omega) = k^2 - k_1^2(i\omega), \tag{10a}$$

$$S^2(k, \omega) = k^2 - k_2^2(i\omega), \tag{10b}$$

and

$$k_1(i\omega) = \frac{\omega}{c_1(i\omega)}, \tag{11a}$$

$$k_2(i\omega) = \frac{\omega}{c_2(i\omega)}. \tag{11b}$$

The boundary conditions to be satisfied at the free surface ($z = 0$) of the medium are

$$(\sigma_z)_{z=0} = \lambda(i\omega) \nabla^2 \phi + 2\mu(i\omega) \frac{\partial u_z}{\partial z} = -p(r, t), \tag{12}$$

and

$$(\tau_{rz})_{z=0} = \mu(i\omega) \left(\frac{\partial u_r}{\partial z} + \frac{\partial u_z}{\partial r} \right) = 0 \tag{13}$$

where u_z, u_r are displacements in the z (downward) and r (radial outward) directions respectively, and $p(r, t)$ is the applied vertical surface load.*

Since u_z is related to the potential functions by

$$u_z = \frac{\partial \phi}{\partial z} - \frac{\partial^2 \psi}{\partial r^2} - \frac{1}{r} \frac{\partial \psi}{\partial r}, \tag{14}$$

*For our present interest we consider only loadings normal to the free surface of the medium, though other modes of loadings may be treated in a similar fashion.

eq 12 can be rewritten as

$$\rho \frac{\partial^2 \phi}{\partial t^2} - 2\mu(i\omega)\left[\frac{1}{r}\frac{\partial \phi}{\partial r} + \frac{\partial^2 \phi}{\partial r^2}\right] - 2\mu(i\omega)\left[\frac{1}{r}\frac{\partial^2 \psi}{\partial z \partial r} + \frac{\partial^3 \psi}{\partial z \partial r^2}\right] = -p(r, t). \tag{15}$$

Transforming eq 15 first with respect to t and then to r, we find

$$[2k^2 - k_2^2(i\omega)]\,\Phi(k, z, \omega) + 2k^2 \frac{\partial \Psi(k, z, \omega)}{\partial z} = -\frac{P(k, \omega)}{\rho\, c_2^2(i\omega)}. \tag{16}$$

Using the relation

$$u_r = \frac{\partial \phi}{\partial r} + \frac{\partial^2 \psi}{\partial z \partial r} \tag{17}$$

and eq 14, eq 13 can be written as

$$\frac{\partial^2 \phi}{\partial z \partial r} + \frac{\partial^3 \psi}{\partial z^2 \partial r} + \frac{\partial^2 \phi}{\partial r \partial z} - \frac{\partial^3 \psi}{\partial r^3} - \frac{\partial}{\partial r}\left(\frac{1}{r}\frac{\partial \psi}{\partial r}\right) = 0. \tag{18}$$

Integrating eq 18 once with respect to r and then applying the Fourier and Hankel transform, we get

$$2\frac{\partial \Phi(k, z, \omega)}{\partial z} + \frac{\partial^2 \Psi(k, z, \omega)}{\partial z^2} + k^2 \Psi(k, z, \omega) = 0. \tag{19}$$

Substituting eq 8 and 9 in eq 16 and 19, we obtain

$$[2k^2 - k_2^2(i\omega)]\,A(k, \omega) - 2sk^2 B(k, \omega) = -\frac{1}{\rho C_2^2(i\omega)} \tag{20}$$

and

$$-2qA(k, \omega) + [2k^2 - k_2^2(i\omega)]\,B(k, \omega) = 0. \tag{21}$$

Solving eq 20 and 21, the expressions for Φ and Ψ then become

$$\Phi(k, z, \omega) = -\frac{[2k^2 - k_2^2(i\omega)]}{\rho\, c_2^2(i\omega)} \frac{P(k, \omega)}{F(k, \omega)} e^{-qz} \tag{22}$$

$$\Psi(k, z, \omega) = -\frac{2q}{\rho\, c_2^2(i\omega)} \frac{P(k, \omega)}{F(k, \omega)} e^{-sz} \tag{23}$$

where

$$F(k, \omega) = [2k^2 - k_2^2(i\omega)]^2 - 4qs\,k^2 \tag{24}$$

is the well known Rayleigh's function.

To obtain ϕ and ψ, we invert eq 22 and 23 and get

$$\phi(r, z, t) = -\frac{1}{2\pi} \int_{-\infty}^{\infty} \int_{0}^{\infty} \frac{[2k^2 - k_2^2(i\omega)]\, P(k, \omega)}{\rho\, c_2^2(i\omega)\, F(k, \omega)} e^{-qz + i\omega t} J_0(kr)\, k dk d\omega \tag{25}$$

and

$$\psi(r, z, t) = -\frac{1}{2\pi} \int_{-\infty}^{\infty} \int_{0}^{\infty} \frac{2q\, P(k, \omega)}{\rho\, c_2^2(i\omega)\, F(k, \omega)} e^{-sz + i\omega t} J_0(kr)\, k dk d\omega . \tag{26}$$

These are the expressions for the potential functions in integral form. To find the response of the medium to the surface loading, we substitute eq 25 and 26 in eq 17 and obtain

$$u_r = \frac{1}{2\pi} \int_{-\infty}^{\infty} \int_{0}^{\infty} \frac{\{[2k^2 - k_2^2(i\omega)]\, e^{-qz} - 2qs\, e^{-sz}\}}{F(k, \omega)} \frac{P(k, \omega)}{\mu(i\omega)} e^{i\omega t} J_1(kr)\, k^2 dk d\omega . \tag{27}$$

Similarly, the expression for the vertical displacement is

$$u_z = \frac{1}{2\pi} \int_{-\infty}^{\infty} \int_{0}^{\infty} \frac{\{[2k^2 - k_2^2(i\omega)]\, q\, e^{-qz} - 2qk^2\, e^{-sz}\}}{F(k, \omega)} \frac{P(k, \omega)}{\mu(i\omega)} e^{i\omega t} J_0(kr)\, k dk d\omega . \tag{28}$$

It is seen that the displacements at given points are functions of the material properties of the medium and the applied load function $P(k, \omega)$. In order to establish a technique of using the measurable displacements for determining the material constants we shall investigate a few assumed loading conditions in the following sections.

PART I: FAR FIELD SURFACE MOTION

A single oscillating source

We first consider the case of a concentrated periodic force applied on the surface of the medium. If the origin of the r-Z axis is chosen to coincide with the load point, we may write

$$p(r, t) = \frac{P_0}{2\pi r} \delta(r)\, e^{i\zeta t} \tag{29}$$

with P_0 being the amplitude of the oscillation, ζ the oscillating frequency and $\delta(r)$ the Dirac delta function.

The Fourier and Hankel transform of eq 29 is

$$P(k,\omega) = P_0\,\delta(\omega - \zeta). \tag{30}$$

Substituting eq 30 in eq 27 and performing the integration for ω, we get

$$u_r = \frac{P_0 e^{i\zeta t}}{2\pi\mu(i\zeta)} \int_0^\infty \left\{ \frac{[2k^2 - k_2^2(i\zeta)]\, e^{-q'z} - 2q's' e^{-s'z}}{[2k^2 - k_2^2(i\zeta)]^2 - 4k^2 q's'} \right\} J_1(kr)\, k^2\, dk \tag{31}$$

where

$$q' = [k^2 - k_1^2(i\zeta)]^{1/2} \tag{32a}$$

and

$$S' = [k^2 - k_2^2(i\zeta)]^{1/2}. \tag{32b}$$

Similarly,

$$u_z = \frac{P_0 e^{i\zeta t}}{2\pi\mu(i\zeta)} \int_0^\infty \left\{ \frac{[2k^2 - k_2^2(i\zeta)]\, q' e^{-q'z} - 2q'k^2 e^{-s'z}}{[2k^2 - k_2^2(i\zeta)]^2 - 4k^2 q's'} \right\} J_0(kr)\, k\, dk. \tag{33}$$

For convenience, we replace ζ by ω and rewrite eq 31 and 33 as

$$u_r = \frac{P_0 e^{i\omega t}}{2\pi\mu(i\omega)} \int_0^\infty \frac{\{[2k^2 - k_2^2(i\omega)]\, e^{-qz} - 2qs\, e^{-sz}\}}{F(k)} J_1(kr)\, k^2\, dk \tag{34}$$

$$u_z = \frac{P_0 e^{i\omega t}}{2\pi\mu(i\omega)} \int_0^\infty \frac{\{[2k^2 - k_2^2(i\omega)]\, q e^{-qz} - 2qk^2 e^{-sz}\}}{F(k)} J_0(kr)\, k\, dk. \tag{35}$$

Since our interest is the surface measurements, we let $z = 0$ and obtain the surface motions

$$u_r(0) = \frac{P_0 e^{i\omega t}}{2\pi\mu(i\omega)} \int_0^\infty \frac{[2k^2 - k_2^2(i\omega) - 2qs]}{F(k)} J_1(kr)\, k^2\, dk \tag{36}$$

$$u_z(0) = -\frac{P_0 e^{i\omega t}}{2\pi\mu(i\omega)} \int_0^\infty \frac{k_2^2(i\omega)\, q}{F(k)} J_0(kr)\, k\, dk. \tag{37}$$

Before performing the integration of the above equations, we note that the positive sign in front of the square root of

$$q(k,\omega) \quad \pm \sqrt{k^2 - k_1^2(i\omega)}$$

and

$$s(k, \omega) = \pm \sqrt{k^2 - k_2^2(i\omega)}$$

should be used in order not to have infinite values for the potential functions Φ and Ψ, eq 8 and 9, as z approaches ∞. Hence the quantity

$$\frac{k\, k_2^2(i\omega)\, q}{F(k)} \tag{38}$$

of the integrand is an odd function of k and if we use the relationship

$$J_0(kr) = \frac{1}{2}\,[H_0^{(1)}(kr) + H_0^{(2)}(kr)] \tag{39}$$

the integral of eq 37 can be written as

$$I = \frac{1}{2} \int_{-\infty}^{\infty} \frac{k\, k_2^2\, q}{F(k)}\, H_0^{(1)}(kr)\, dk \tag{40}$$

where $H_0^{(1)}$ denotes the Hankel function of the first kind of zero order, and $H_0^{(2)}$ the second kind of zero order.

Changing the variable of integration from k to a complex variable $\xi = k + i\tau$, we may follow the route* as indicated in Figure 1 for contour integration in ξ-plane. Noting that for large argument

$$H_0^{(1)}(\xi r) \sim \sqrt{\frac{2}{\pi \xi r}}\, \exp\,[i(\xi r - \frac{\pi}{4})], \tag{41a}$$

$$H_0^{(2)}(\xi r) \sim \sqrt{\frac{2}{\pi \xi r}}\, \exp\,[-i(\xi r - \frac{\pi}{4})], \tag{41b}$$

the integrand vanishes on the infinite arc and we get

$$I = -\pi i\, \frac{\kappa\, k_2^2\, q(\kappa)}{F'(\kappa)}\, H_0^{(2)}(\kappa r) - \int_{L_1} - \int_{L_2} \tag{42}$$

where $\int_{L_1}$ and $\int_{L_2}$ are the line integrals of the function along the cuts L_1 and L_2 respectively, κ is the Rayleigh pole, F' is the derivative of F with respect to k.

The first term on the right-hand side of eq 42 represents the Rayleigh (surface) wave effect, while the branch line integrals are the effects of the dilatational waves and shear waves

*Since both k_1 and k_2 are complex numbers of ω with Re $\omega > 0$, the branch cuts are parts of hyperbolas as shown in the figure.

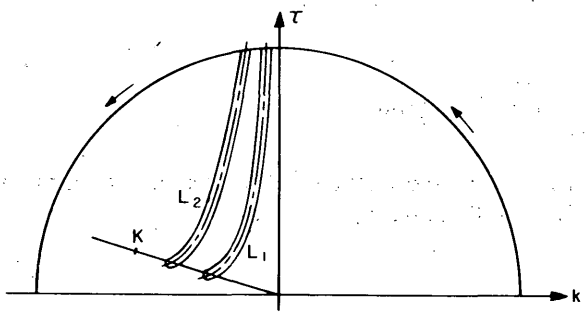

Figure 1. Integration contour in complex ξ-plane.

Table I. Comparison* of surface vibrations from dilatational waves and shear waves with those from Rayleigh waves, as a function of location (κr) and Poisson's ratio (ν).

ν	κr	$\frac{\text{Dilatational term}}{\text{Rayleigh term}}$ (%)	$\frac{\text{Shear term}}{\text{Rayleigh term}}$ (%)
1/4	10	0.38477	0.00405
	20	0.00067	-
0.30	10	0.34050	0.00431
	20	0.00078	-
1/3	10	0.32880	0.00465
	20	0.00109	-

*Values of $\int_{L_1}$ and $\int_{L_2}$ are computed by the method of steepest descent.

respectively. As shown in Table I, the effect of the first term predominates the far field and we may omit those of the second and third terms.

Hence, in far field we write

$$u_z(0) = i \frac{P_0 e^{i\omega t}}{2\mu(i\omega)} \frac{\kappa k_2^2 q(\kappa)}{F'(\kappa)} H_0^{(2)}(\kappa r). \tag{43}$$

Using the asymptotic expansion of $H_0^{(2)}$ for large κr (eq 41b) we get

$$u_z(0) = -\frac{P_0}{\mu(i\omega)} \left(\frac{1}{2\pi\kappa r}\right)^{1/2} \frac{\kappa k_2^2 q(\kappa)}{F'(\kappa)} \exp\left[i(\omega t - \kappa r - \frac{\pi}{4})\right]. \tag{44}$$

Similarly, it can be shown that

$$u_r(0) = i \frac{P_0}{\mu(i\omega)} \left(\frac{1}{2\pi\kappa r}\right)^{1/2} \frac{\kappa^2[2\kappa^2 + k_2^2 - 2q(\kappa)s(\kappa)]}{F'(\kappa)} \exp\left[i(\omega t - \kappa r - \frac{\pi}{4})\right]. \tag{45}$$

It is seen that the amplitude of the surface motion decays with distance r according to $1/\sqrt{r}$ and travels with the surface velocity C_R as κ is the ratio of frequency ω and C_R.

To find the attenuation effect of the medium, we let

$$k_R = \frac{C_R}{C_2}.$$

Then*

$$C_R(i\omega) = k_R(\nu)\sqrt{\frac{\mu(i\omega)}{\rho}}, \tag{46}$$

and

$$\kappa(i\omega) = \frac{\omega}{C_R(i\omega)} = \frac{\omega}{k_R(\nu)\,(M_2^*/\rho)^{1/2}\sec(\theta_2/2)}\left(1 - i\tan\frac{\theta_2}{2}\right) \tag{47}$$

where

$$M_2^* = (\mu'^2 + \mu''^2)^{1/2}, \tag{48a}$$

$$\tan\theta_2 = \frac{\mu''}{\mu'}, \tag{48b}$$

and μ' and μ'' are the real and imaginary parts of $\mu(i\omega)$ as defined before.

Thus, if we write

$$\frac{\omega}{C_R(i\omega)} \equiv \left(\frac{\omega}{C_R} - i\alpha_2\right), \tag{49}$$

we get

$$C_R = k_R(\nu)\left(\frac{M_2^*}{\rho}\right)^{1/2}\sec\frac{\theta_2}{2}, \tag{50a}$$

and α_2 = the attenuation factor

$$\alpha_2 = \frac{\omega}{C_R}\tan\frac{\theta_2}{2}. \tag{50b}$$

*As shown in elastic theory, $k_R(\nu)$ is a function of Poisson's ratio ν. Its value varies from 0.875 to 0.955 when ν changes from 0 to 0.5. Since we are not certain how ν varies with frequency, and since the frequency range involved in the present study is quite limited, we may assume that $k_R(\nu)$ is independent of frequency.

Using eq 49, the displacement functions can be rewritten as

$$u_z(0) = \frac{P_0 K_z \kappa(i\omega)}{\mu(i\omega)} \left(\frac{1}{2\pi\kappa(i\omega)r}\right)^{1/2} \exp(-a_2 r) \exp\left[i\omega\left(t - \frac{r}{C_R}\right) - i\frac{\pi}{4}\right], \tag{51}$$

$$u_r(0) = -i\frac{P_0 K_r \kappa(i\omega)}{\mu(i\omega)} \left(\frac{1}{2\pi\kappa(i\omega)r}\right)^{1/2} \exp(-a_2 r) \exp\left[i\omega\left(t - \frac{r}{C_R}\right) - i\frac{\pi}{4}\right], \tag{52}$$

where

$$K_z = -\frac{k_2^2 q(\kappa)}{F'(\kappa)} \tag{53a}$$

$$K_r = -\frac{\kappa[2\kappa^2 + k_2^2 - 2q(\kappa)s(\kappa)]}{F'(\kappa)} \tag{53b}$$

are functions* of ν, the Poisson's ratio.

Thus, we see in a viscoelastic medium the amplitudes are further reduced exponentially with distance by a factor related to the dissipative property of the medium.

If we choose two reference points in the far field of distances r_1 and r_2 from the source, respectively, and take the ratio of the vibration amplitudes of these points, then the resultant quantity has a rather simple expression and becomes

$$\left.\begin{aligned} R_{1,2} &= \left|\frac{u_{z1}(0)}{u_{z2}(0)}\right| \\ &= \left(\frac{r_2}{r_1}\right)^{1/2} \exp[a_2(r_2 - r_1)], \end{aligned}\right\} \tag{54}$$

as the other terms are not a function of r and thus do not change with the location. Since r_1 and r_2 are known, if the value of $R_{1,2}$ is measured it is not difficult to determine a_2 from eq 54.

The phase shift χ between the points may be given as

$$\chi_{1,2} = \frac{\omega}{C_R}(r_2 - r_1). \tag{55}$$

If we select points 1 and 2 with a phase shift of 2π, we get from eq 55

$$C_R = f d_{1,2} \tag{56}$$

*These are again under the assumption that $k_R(\nu)$ is independent of frequency, as mentioned earlier. It is assumed also that the ratio C_1 to C_2 is not affected by frequency changes in the test range.

where $d_{1,2}$ is the distance between the selected points and f is the vibration frequency. Thus, surface wave velocity may be determined through observations of phase shift between selected points.*

Since in field practice vibration is generally transmitted through the base of a vibrator, load is actually applied to the ground on a finite area rather than at a single concentrated point. Therefore, there will be an influence on the displacement functions arising from the characteristics associated with the area and shape of the base plate and the pressure distribution beneath the plate. This will be investigated in some detail by considering several types of input sources with variety in their amplitudes and size expressed in terms of nondimensional quantity.

A group of forces over a finite area

As most of the vibrators are equipped with circular bases, it may be proper to consider only the possible load distributions over a circular area. For this purpose, we take the following three cases of forces which are distributed:

1) uniformly over the area

2) as a parabola

3) as the reaction under a rigid plate (approximation).

For case 1, we let the radius of the circle be r_0 and the applied load be p_0. Then the load function may be represented by

$$p(r,t) = p_0 e^{i\zeta t} [h(r) - h(r - r_0)] \tag{57}$$

where $h(...)$ is the Heaviside step function.

The Fourier and Hankel transform of eq 57 is

$$P(k,\omega) = 2\pi r_0 p_0 \delta(\omega - \zeta) \frac{J_1(kr_0)}{k}. \tag{58}$$

Substituting eq 58 into the expressions for the displacement functions u_r and u_z (eq 27 and 28) and replacing ζ by ω after integration, we get

$$u_{ru} = \frac{p_0 r_0 e^{i\omega t}}{\mu(i\omega)} \int_0^\infty \frac{[(2k^2 - k_2^2) e^{-qz} - 2qs e^{-sz}]}{F(k)} J_1(kr_0) J_1(kr) k dk \tag{59}$$

and

$$u_{zu} = \frac{p_0 r_0 e^{i\omega t}}{\mu(i\omega)} \int_0^\infty \frac{[(2k^2 - k_2^2) q e^{-qt} - 2qk^2 e^{-sz}]}{F(k)} J_1(kr_0) J_0(kr) dk. \tag{60}$$

*This was the technique used by the U.S. Army Waterways Experiment Station soil dynamics group in field observations of surface velocity and, subsequently, for the determination of elastic modulus of soils. Detailed procedure can be found in the report by Z.B. Fry, *A Procedure for Determining Elastic Moduli of Soils by Field Vibratory Techniques*, USAE WES Miscellaneous Paper 4-577, June 1963.

At the surface then they reduce to

$$u_{ru}(0) = \frac{p_0 r_0 e^{i\omega t}}{\mu(i\omega)} \int_0^\infty \frac{(2k^2 - k_2^2 - 2qs)}{F(k)} J_1(kr_0) J_1(kr)\, kdk \tag{61}$$

$$u_{zu}(0) = -\frac{p_0 r_0 e^{i\omega t}}{\mu(i\omega)} \int_0^\infty \frac{k_2^2 q}{F(k)} J_1(kr_0) J_0(kr)\, dk . \tag{62}$$

Using techniques similar to those outlined in the last section, and noting that for large ξ

$$J_1(\xi r_0) H_0^{(1)}(\xi r) \sim \frac{1}{\pi \xi (r r_0)^{1/2}} \left[e^{(r+r_0)(-\tau \pm ik)} + e^{(r-r_0)(-\tau \pm ik)} \right] \tag{63}$$

we get,* in far field $r > r_0$,

$$u_{zu}(0) = \frac{p_0 r_0}{\mu(i\omega)} K_z J_1(kr_0) \sqrt{\frac{2\pi}{\kappa r}} \exp(-a_2 r) \exp\left[i\omega \left(t - \frac{r}{C_R} \right) - i \frac{\pi}{4} \right]. \tag{64}$$

Here again, the effect of the two branch line integrals has been neglected.

Comparing eq 64 with eq 51, there is a new factor $J_1(\kappa r_0)$, replacing κ, appearing in $u_{zu}(0)$ due to the assumed load distribution. Since the Bessel function has zero roots for real arguments, there will be frequencies at which the source will produce no vertical surface motion in the far field. Physically, it may be interpreted as the vibration effects produced by each individual element of the source which cancel each other at these critical frequencies. However, if the ground behaves viscoelastically, i.e., involving dissipation of energy, the arguments of the previously mentioned Bessel function are complex and therefore motions will be reduced to minimum magnitudes, rather than zero, at these critical frequencies.

Since other terms are similar to the single concentrated force case, it is expected that the expressions for the Amplitude Ratio $R_{1,2}$ and the phase shift $\chi_{1,2}$ are of the same form as given by eq 54 and 55. Hence, the techniques for determining the surface wave velocity and the attenuation factor can also be applied for the uniformly distributed input source over a circular area.

For the remaining two cases of load distributions we let

$$p_p(r, t) = \frac{2P_0(r_0^2 - r^2)}{\pi r_0^4} e^{i\zeta t} [h(r) - h(r - r_0)], \tag{65}$$

$$p_R(r, t) = \frac{P_0}{2\pi r_0} \frac{1}{\sqrt{r_0^2 - r^2}} e^{i\zeta t} [h(r) - h(r - r_0)], \tag{66}$$

*The integration of eq 61 for $u_{ru}(0)$ can be handled in a similar way. Since field measurements are normally concerned with only vertical displacements, this part is omitted. Also, for simplicity, $\kappa(i\omega)$ is written as κ.

and obtain

$$P_p(k,\omega) = 8P_0\,\delta(\omega - \zeta)\frac{J_2(kr_0)}{(kr_0)^2}, \tag{67}$$

$$P_R(k,\omega) = P_0\,\delta(\omega - \zeta)\frac{\sin kr_0}{kr_0}, \tag{68}$$

where P_0 is the total load* and the subscript under the load function on the left-hand side of the equation refers to the types of the assumed load distribution.

Hence, the corresponding displacement functions are

$$u_{rp} = \frac{4P_0 e^{i\omega t}}{\pi r_0^2 \mu(i\omega)} \int_0^\infty \frac{[(2k^2 - k_2^2)e^{-qz} - 2qs\,e^{-sz}]}{F(k)} J_2(kr_0)J_1(kr)\,dk \tag{69}$$

$$u_{zp} = \frac{4P_0 e^{i\omega t}}{\pi r_0^2 \mu(i\omega)} \int_0^\infty \frac{[(2k^2 - k_2^2)q\,e^{-qz} - 2qk^2 e^{-sz}]}{kF(k)} J_2(kr_0)J_0(kr)\,dk \tag{70}$$

$$u_{rR} = \frac{P_0 e^{i\omega t}}{2\pi r_0 \mu(i\omega)} \int_0^\infty \frac{[(2k^2 - k_2^2)e^{-qz} - 2qs\,e^{-sz}]}{F(k)} \sin(kr_0)J_1(kr)\,kdk \tag{71}$$

and

$$u_{zR} = \frac{P_0 e^{i\omega t}}{2\pi r_0 \mu(i\omega)} \int_0^\infty \frac{[(2k^2 - k_2^2)q\,e^{-qz} - 2qk^2 e^{-sz}]}{F(k)} \sin(kr_0)J_0(kr)\,dk. \tag{72}$$

For vertical surface displacements, we have

$$u_{zp}(0) = -\frac{4P_0 e^{i\omega t}}{\pi r_0^2 \mu(i\omega)} \int_0^\infty \frac{k_2^2 q}{kF(k)} J_2(kr_0)J_0(kr)\,dk \tag{73}$$

and

$$u_{zR}(0) = -\frac{P_0 e^{i\omega t}}{2\pi r_0 \mu(i\omega)} \int_0^\infty \frac{k_2^2 q}{F(k)} \sin(kr_0)J_0(kr)\,dk. \tag{74}$$

*Note that p_0 has been changed to P_0 as it is the more appropriate symbol for total force.

Proceeding with the technique of previous sections, the equations above can be shown to become

$$u_{zp}(0) = \frac{4P_0}{r_0^2 \mu(i\omega)} K_z \frac{J_2(\kappa r_0)}{\kappa} \sqrt{\frac{2}{\pi \kappa r}} \exp(-\alpha_2 r) \exp\left[i\omega\left(t - \frac{r}{C_R}\right) - i\frac{\pi}{4}\right], \quad (75)$$

and

$$u_{zR}(0) = \frac{P_0 K_z}{r_0 \mu(i\omega)} \sin(\kappa r_0) \sqrt{\frac{1}{2\pi\kappa r}} \exp(-\alpha_2 r) \exp\left[i\omega\left(t - \frac{r}{C_R}\right) - i\frac{\pi}{4}\right], \quad (76)$$

in the far field when the effects of the branch line integrals are neglected.

Here again we notice that the functions $J_2(\kappa r_0)$ and $\sin \kappa r_0$ will produce zero vibration amplitudes at some critical frequencies for *elastic* media. Hence, all critical frequencies are determined from zeros of the Bessel or circular functions. Let X_n be the nth root* of these functions. Then we get

$$f_n = \frac{C_R X_n}{2\pi r_0} \quad \text{or} \quad C_R = \frac{2\pi f_n r_0}{X_n}. \quad (77)$$

Thus, knowing the surface wave velocity (or dispersion curve), one may predict the critical frequencies from eq 77; or, by observing these frequencies, the velocity may be calculated.

However, as mentioned earlier, when dissipation is involved there will be no *zero* ground motions but rather the *minima*. The value of the minima may be determined from the amplitude terms of eq 64, 75 and 76. Hence, when damping is present, it will cause a shift in critical frequencies. Furthermore, these frequencies also depend upon the *location* of the observations made as they all have the square root and exponential terms of r. Taking $r/r_0 = 10$ and 20, we made computations for the first two roots of the minima of all three assumed load distributions. These values are listed in Table II. We notice that the shift in frequencies is not great for the values investigated.† Thus, within experimental error, eq 77 is still useful for the case of small magnitude of damping.

While the magnitudes of the minima are too small for any helpful information, those of the maxima are of considerable interest. Setting $r/r_0 = 10$, their values (scaled magnitudes) and the corresponding (scaled) frequencies are calculated in Table III for a variety of damping coefficients. Also, the magnitudes of the surface vibration, in the vicinity of the first maximum, vs the damping effect of the ground are illustrated in Figures 2-4. Though the peaks indicated on these figures are not very sharp, the corresponding critical frequencies can be located with good accuracy.**

Let $M_{1,2}$ be the ratio of the magnitude of the first observed maximum to that of the second maximum. A set of curves showing the effect of damping on these ratios is given in Figure 5. It is seen that the values of $M_{1,2}$ change rapidly with the change in values of $\tan(\theta_2/2)$. Hence, they are sensitive indicators of the damping magnitude of the ground.

---

*Values of the zero roots for Bessel functions may be found in tables, for example, E. Jahnke and F. Emde, *Table of Functions*, Dover Publication. First three roots of J_1 are: $X_1 = 3.832$, $X_2 = 7.016$, and $X_3 = 10.173$; and those for J_2 are: $X_1 = 5.135$, $X_2 = 8.417$, and $X_3 = 11.620$.

†For greater distance and higher damping values, the amplitudes are too small to distinguish the minimum.

**Since their magnitudes do not change rapidly in the vicinity of the maxima, the measured values are quite close to the true peak values even if not actually at the peak.

Table II. Vibration frequencies, at minimum amplitudes, as a function of observation location (r/r_0), damping magnitude ($\tan \theta_2/2$) and input load distribution: 1) uniform, 2) parabolic, and 3) rigid plate approximation.

n	$\frac{r}{r_0}$	$\tan\frac{\theta_2}{2}$	$X_n = \kappa r_0 \left(= \frac{2\pi f_n r_0}{C_R}\right)$		
			(1)	(2)	(3)
1	10	0	3.8317	5.1356	3.1416
		0.02	3.8336	5.1408	3.1418
		.04	3.8443	5.1658	3.1454
		.06	3.8723	5.2322	3.1577
	20	0	3.8317	5.1356	3.1416
		0.02	3.8348	5.1430	3.1426
		.04	3.8543	5.1854	3.1519
		.06	3.9143	-	3.1822
2	10	0	7.0156	8.4172	6.2832
		0.02	7.0210	8.4280	6.2851
		.04	7.0542	8.4880	6.3040
		.06	7.1582	8.7310	6.3671
	20	0	7.0156	8.4172	6.2832
		0.02	7.0250	8.4340	6.2883
		.04	7.0920	8.5539	6.3325
		.06	-	-	-

Table III. Maximum vibration amplitudes and their corresponding frequencies at r/r_0 = 10 for input load distributions: 1) uniform, 2) parabolic and 3) rigid plate approximation.

$\tan\frac{\theta_2}{2}$	(1)		(2)		(3)	
	$\frac{\omega r_0}{C_R}$	$(Amp_1)_{max}$	$\frac{\omega r_0}{C_R}$	$(Amp_2)_{max}$	$\frac{\omega r_0}{C_R}$	$(Amp_3)_{max}$
.00	5.2335	0.11937	6.4598	0.01856	4.6042	0.05847
.01	5.1331	.07118	6.3579	.00980	4.5044	.03712
.02	5.0366	.04298	6.2609	.00525	4.4080	.02385
.03	4.9452	.02627	6.1679	.00285	4.3152	.01550
.04	4.8566	.01625	6.0739	.00157	4.2262	.01019
.05	4.7704	.01017	5.9769	.00088	4.1403	.00678
.06	4.6849	.00644	5.8707	.00050	4.0572	.00456
.07	4.5967	.00415	5.7417	.00029	3.9751	.00310
.08	4.5019	.00270	-	-	3.8927	.00214
.09	4.3886	.00179	-	-	3.8070	.00149

Where $Amp_1 = \frac{\mu}{p_0 r_0 K_z} u_z(0)$ $\quad Amp_2 = \frac{r_0 \mu}{P_0 K_z} u_z(0)$ $\quad Amp_3 = \frac{r_0 \mu}{P_0 K_z} u_z(0)$

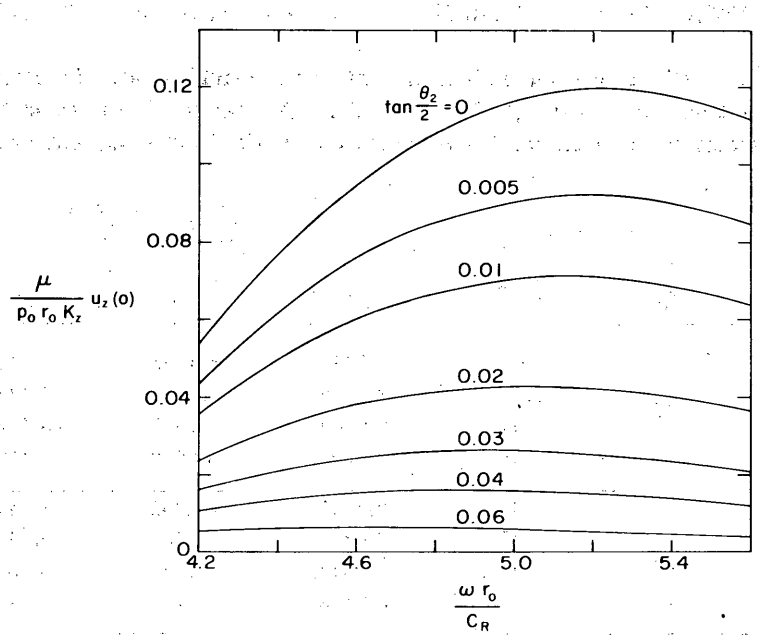

Figure 2. Vibration amplitude vs frequency, near first maximum, at $r/r_0 = 10$ and with uniform loading.

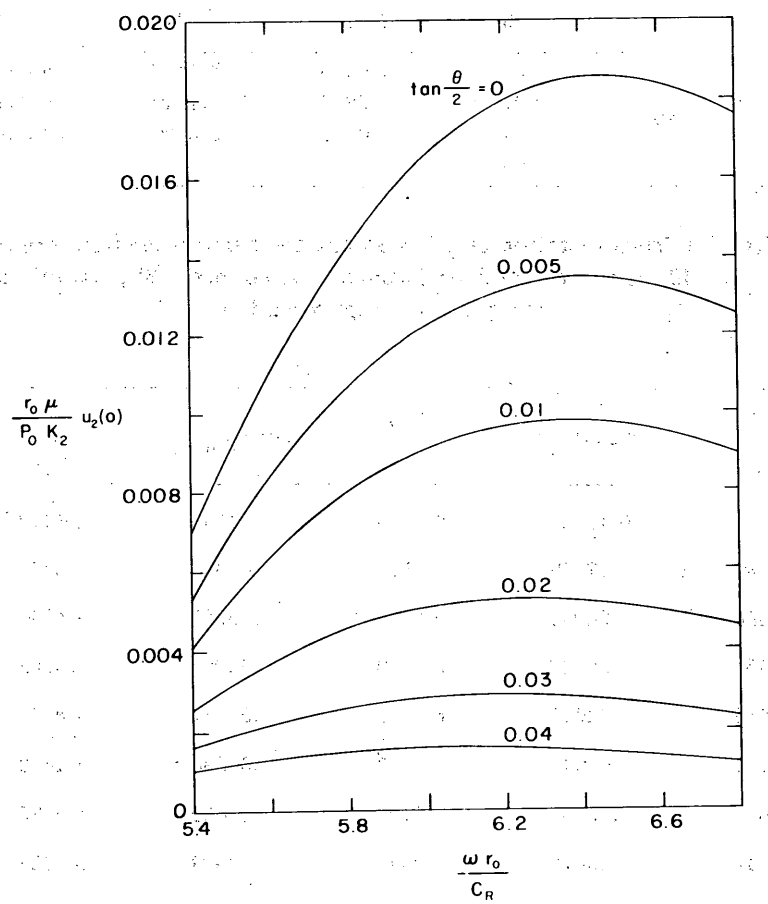

Figure 3. Vibration amplitude vs frequency, near first maximum, at $r/r_0 = 10$ and with parabolic loading.

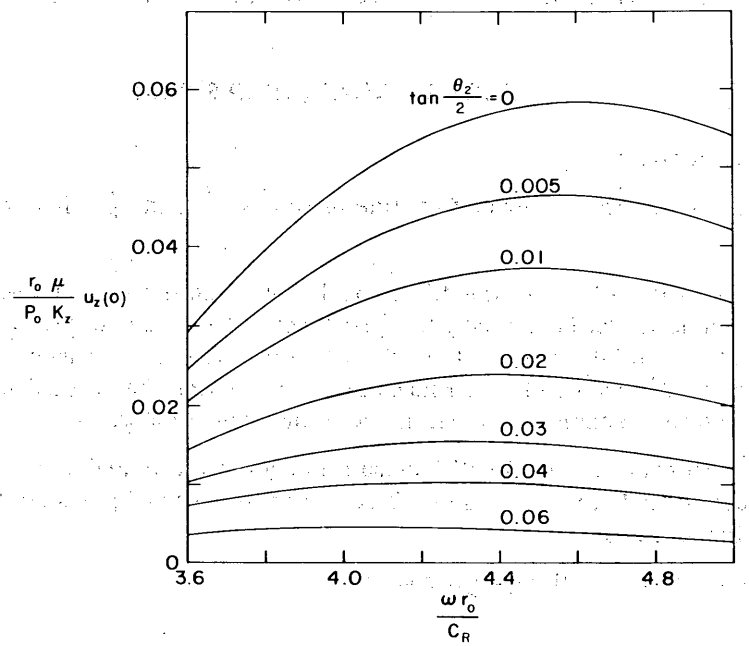

Figure 4. Vibration amplitude vs frequency, near first maximum, at $r/r_0 = 10$ and with loading to approximate rigid plate reaction.

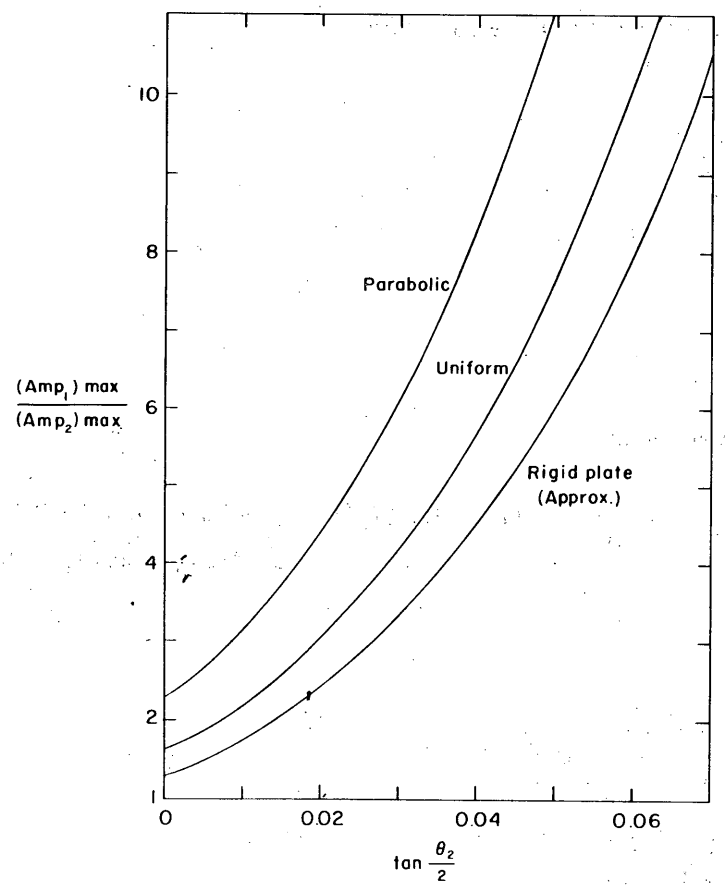

Figure 5. Ratio of first and second maximum amplitudes vs $\tan\theta_2/2$ for three types of input loadings.

PART II: NEAR FIELD STUDY

Motion at center of source

In near field study, the influence from line integrals $\int_{L_1}$ and $\int_{L_2}$ along the branch cuts L_1 and L_2, which represent the effects of the dilatational waves and the shear waves respectively, are important and can no longer be neglected. Furthermore, the method of steepest descent used in Part I to evaluate these integrals is also not applicable. Hence, to compute the surface motion in a near field, we have a choice of either numerically evaluating the original infinite integral or using the contour integration technique and dealing with the branch integrals.

Here, we shall choose to deal with the main integral directly and start the investigation with the uniformly distributed pressure source. The other two cases of pressure distribution will then be handled in a similar manner.

At the center where $r = 0$, eq 62 becomes

$$u_{zu}(0,0,t) = -\frac{p_0 r_0 e^{i\omega t}}{\mu(i\omega)} \int_0^\infty \frac{k_2^2(i\omega)\, q(k)}{F(k)} J_1(k r_0)\, dk \tag{78}$$

where p_0 is the uniformly distributed pressure.

Introducing

$$\xi = \frac{k c_2}{\omega} \tag{79a}$$

and

$$a_0 = \frac{\omega r_0}{c_2}, \tag{79b}$$

eq 78 can be rewritten as*

$$\frac{\rho c_2^2 r_0}{P_0 e^{i\omega t}} u_{zu}(0,0) = -\frac{[1 - i\tan(\theta_2/2)]^4}{\pi} \int_0^\infty \frac{q[\xi, \eta_1, \tan(\theta_1/2), \tan(\theta_2/2)]}{F[\xi, \eta_1, \tan(\theta_1/2), \tan(\theta_2/2)]} J_1(\xi a_0)\, d\xi \tag{80}$$

where

$$c_2 = \left(\frac{M_2^*}{\rho}\right)^{1/2} \sec\frac{\theta_2}{2} \tag{81}$$

$$\eta_1^2 = \frac{(1 - 2\nu)}{2(1 - \nu)}, \tag{82a}$$

*For simplicity, from here on the time dimension t in the displacement function u_z will be omitted.

$$\tan \theta_1 = \frac{(\lambda_1'' + 2\mu'')}{(\lambda_1' + 2\mu')} \cdot \tag{82b}$$

M_2^* and $\tan \theta_2$ are defined by eq 48a, b , ν is the Poisson's ratio of the supporting medium, λ', λ'', and μ', μ'' are the real and imaginary parts of the complex Lame's constants $\lambda(i\omega)$ and $\mu(i\omega)$, as defined early in Part I, and P_0 is the total load applied at the source.

Let g_{1u}, g_{2u} be the real and imaginary parts of the (scaled) complex center motion. Equation 80 may be further written as:

$$U_{zu}(0,0) = g_{1u}\left(\nu, a_0, \tan\frac{\theta_1}{2}, \tan\frac{\theta_2}{2}\right) + i\, g_{2u}\left(\nu, a_0, \tan\frac{\theta_1}{2}, \tan\frac{\theta_2}{2}\right) \tag{83}$$

where

$$U_{zu}(0,0) = \frac{\rho c_2^2 r_0}{P_0 e^{i\omega t}} u_{zu}(0,0)$$

is the (scaled) surface vertical displacement at the center of the circle, under the uniformly distributed pressure.

In this form it is then possible to express the center displacements directly in terms of the four parameters ν, a_0, $\tan \theta_1/2$, and $\tan \theta_2/2$. To illustrate this relationship, we take the cases of ν = 0.25 and 0.5 and plot the computed values of g_{1u} and g_{2u} in Figures 6-11.

It is seen that both g_{1u} and g_{2u} are subjected to the influence of $\tan \theta_1/2$ and $\tan \theta_2/2$, with the exception of ν = 0.5 where $\tan \theta_1/2$ has no effect. The magnitude of their effect, however, varies with the frequency, as represented by a_0. For example, their influence on g_{1u} is more prominent in the high frequency range (i.e. for large a_0 values). As for g_{2u}, on the contrary, it is in the middle and near the lower frequency range where a_0 is approximately equal to 0.5. g_{1u} and g_{2u} also respond differently to the variations in $\tan \theta_1/2$ and $\tan \theta_2/2$. The magnitude of g_{1u} is generally decreased with increased $\tan \theta_1/2$ or $\tan \theta_2/2$ values. In the case of g_{2u}, it first increases in the lower frequency range and then decreases at higher frequencies when the value of $\tan \theta_2/2$ is increased; however, its value is generally increased with increased $\tan \theta_1/2$.

The response of g_{1u} and g_{2u} to vibration frequencies and the damping properties of the supporting medium may be better illustrated and understood by using the analogy of the "mechanical impedance."

Differentiating eq 83 once with respect to t, we get

$$\dot{U}_{zu}(0,0) = \omega\left[-g_{2u}\left(\nu, a_0, \tan\frac{\theta_1}{2}, \tan\frac{\theta_2}{2}\right) + i\, g_{1u}\left(\nu, a_0, \tan\frac{\theta_1}{2}, \tan\frac{\theta_2}{2}\right)\right]. \tag{84}$$

The mechanical impedance may be defined as the ratio of the applied force to the center velocity of the "plate." Let it be denoted by Z. Then,* the mechanical impedance of the medium for a uniformly distributed pressure source is:

*For simplicity, $g_1(\nu, a_0, \tan \theta_1/2, \tan \theta_2/2)$ and $g_{2u}(\nu, a_0, \tan \theta_1/2, \tan \theta_2/2)$ are abbreviated to g_{1u} and g_{2u}.

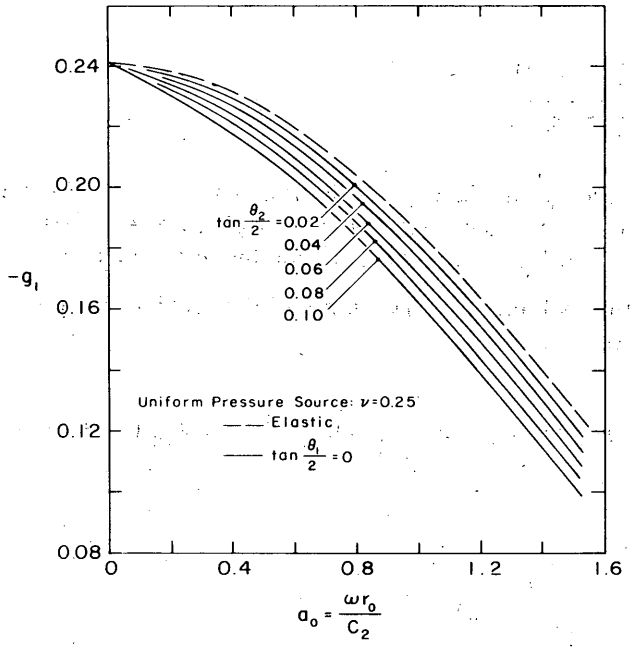

Figure 6. g_1 *vs* a_0 *and* $\tan(\theta_2/2)$.

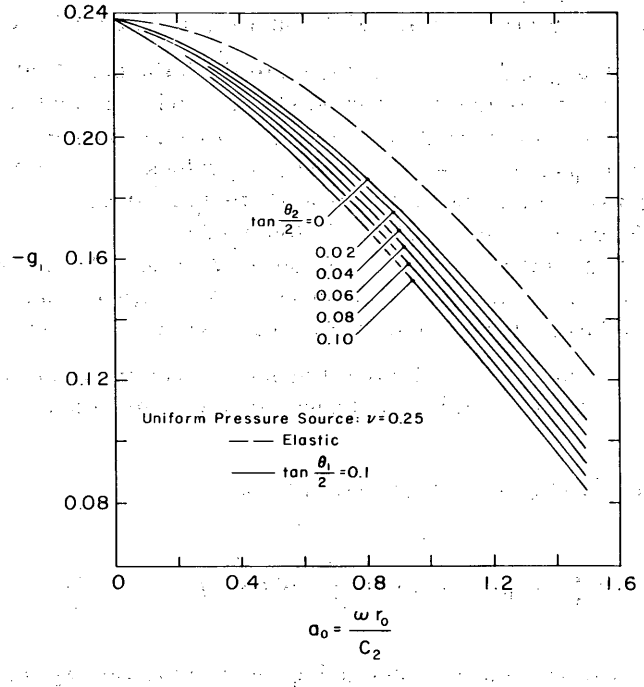

Figure 7. g_1 *vs* a_0 *and* $\tan(\theta_2/2)$.

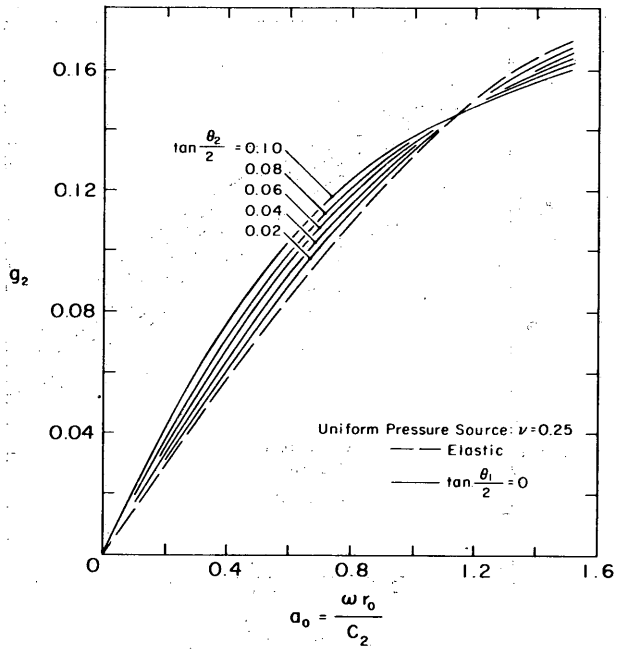

Figure 8. g_2 *vs* a_0 *and* $\tan(\theta_2/2)$.

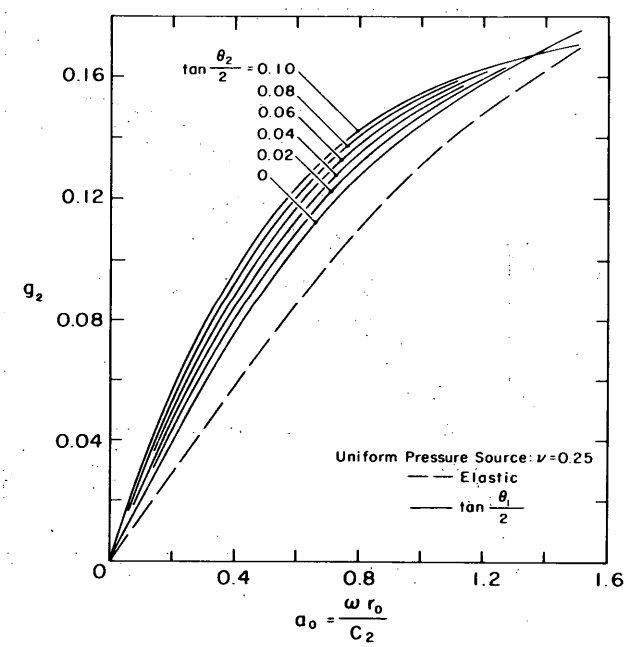

Figure 9. g_2 *vs* a_0 *and* $\tan(\theta_2/2)$.

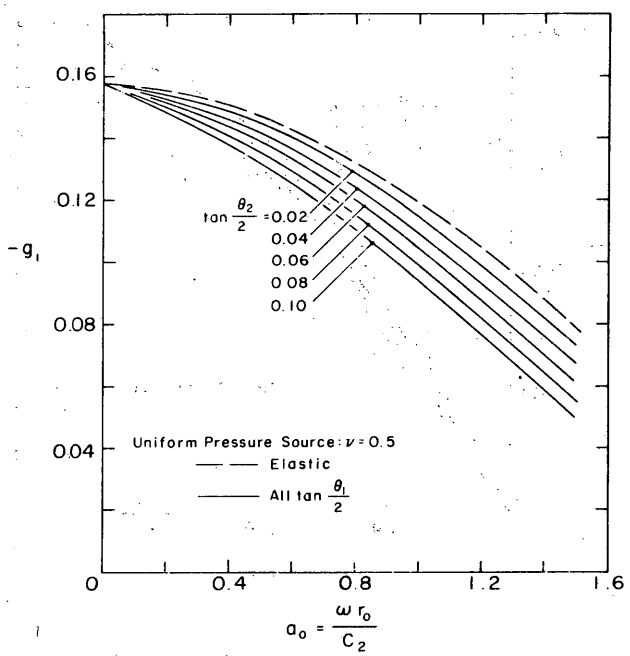

Figure 10. g_1 *vs* a_0 *and* $\tan(\theta_2/2)$.

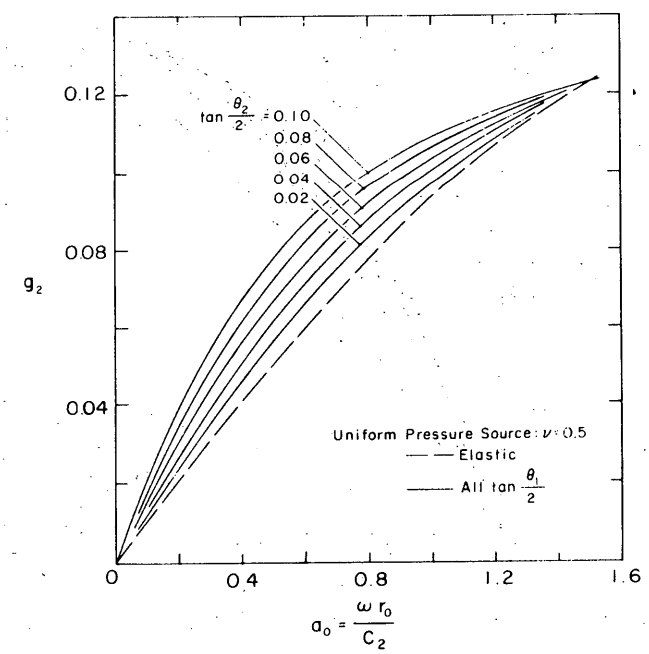

Figure 11. g_2 *vs* a_0 *and* $\tan(\theta_2/2)$.

$$Z_u = i \frac{\rho c_2^2 r_0}{\omega (g_{1u} + i g_{2u})}. \tag{85}$$

The "mechanical resistance" R and the "mechanical reactance" X are readily shown to be

$$R_u = \frac{\rho c_2 r_0^2}{a_0} \frac{g_{2u}}{g_{1u}^2 + g_{2u}^2} \tag{86}$$

and

$$X_u = \frac{\rho c_2 r_0^2}{a_0} \frac{g_{1u}}{g_{1u}^2 + g_{2u}^2}. \tag{87}$$

Hence, it is clear that losses in a medium are related to g_{2u} and the stiffness to g_{1u}. The relation of R_u and X_u to a_0 is shown in Figures 12-14. We see that both X and R are decreasing with increasing a_0. The determination of $\tan \theta_2/2$ from measurements appears to be best accomplished using a low frequency range, i.e. for a_0 less than 0.5.

When the force distribution of the source is in the form of a parabola or as the static reaction under a rigid plate (Rigid Plate Approximation), the surface displacements at $r = 0$ become

$$u_{zp}(0,0,t) = -\frac{4 P_0 e^{i\omega t}}{\pi r_0^2 \mu(i\omega)} \int_0^\infty \frac{k_2^2(i\omega)\, q(k)}{k F(k)} J_2(k r_0)\, dk \tag{88}$$

and

$$u_{zR}(0,0,t) = -\frac{P_0 e^{i\omega t}}{2\pi r_0 \mu(i\omega)} \int_0^\infty \frac{k_2^2(i\omega)\, q(k)}{F(k)} \sin(k r_0)\, dk. \tag{89}$$

Equations 88 and 89 can also be written in the form:

$$U_{zp}(0,0) = g_{1p}\left(\nu, a_0, \tan\frac{\theta_1}{2}, \tan\frac{\theta_2}{2}\right) + i g_{2p}\left(\nu, a_0, \tan\frac{\theta_1}{2}, \tan\frac{\theta_2}{2}\right) \tag{90}$$

and

$$U_{zR}(0,0) = g_{1R}\left(\nu, a_0, \tan\frac{\theta_1}{2}, \tan\frac{\theta_2}{2}\right) + i g_{2R}\left(\nu, a_0, \tan\frac{\theta_1}{2}, \tan\frac{\theta_2}{2}\right) \tag{91}$$

where

$$U_{zp}(0,0) = \frac{\rho c_2^2 r_0}{P_0 e^{i\omega t}} u_{zp}(0,0)$$

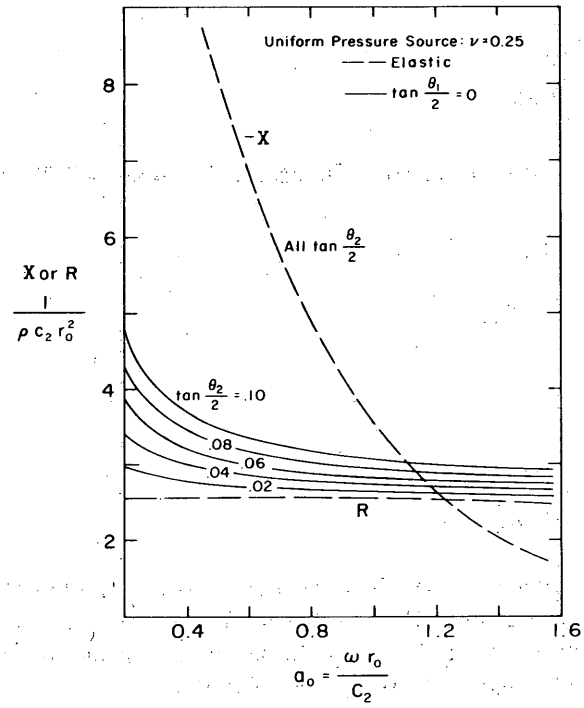

Figure 12. X, R vs a_0 *and* $\tan(\theta_2/2)$.

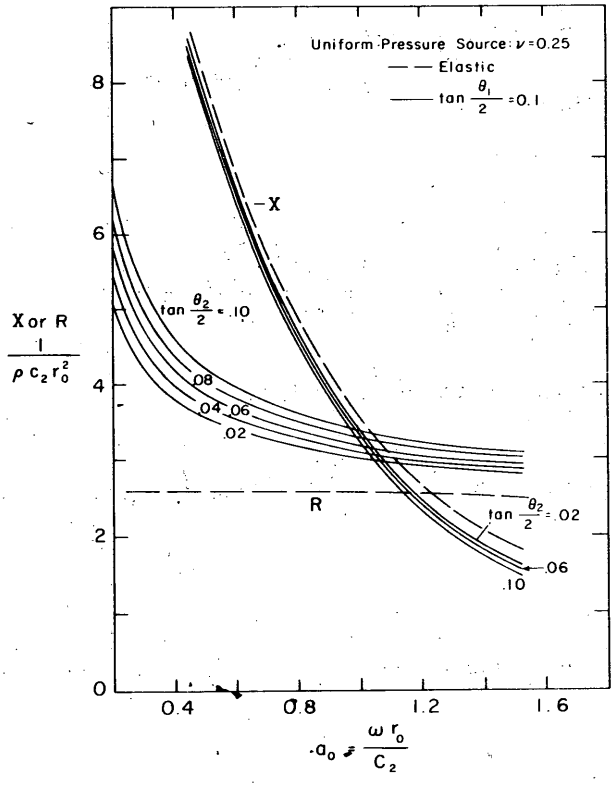

Figure 13. X, R vs a_0 *and* $\tan(\theta_2/2)$.

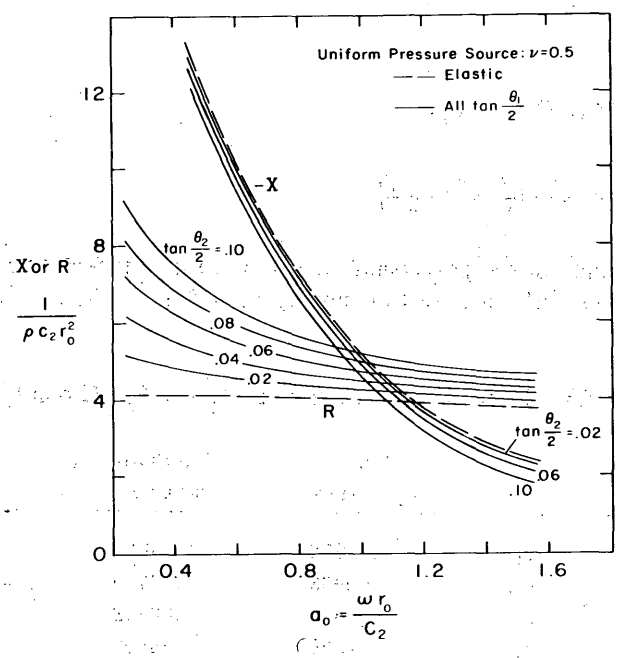

Figure 14. X, R vs a_0 *and* tan $(\theta_2/2)$.

and

$$U_{zR}(0,0) = \frac{\rho c_2^2 r_0}{P_0 e^{i\omega t}} \; u_{zR}(0,0)$$

are the (scaled) center surface vertical displacements with subscripts p and R referring to parabolic and rigid plate approximation pressure distributions, respectively.

The relationships of g_1 and g_2 to the parameters ν, a_0, tan $\theta_1/2$ and tan $\theta_2/2$ for these two pressure distributions can be computed from eq 88 and 89. Since they are similar to those presented for the uniform pressure source case, graphic presentations are omitted. However, their simplified analytical expressions as well as that for the uniform pressure loading will be attempted in the next section.

Approximation of displacements

The numerical procedures used to obtain the relationships of g_1, g_2 with the parameters ν, a_0, tan $(\theta_1/2)$ and tan $(\theta_2/2)$ are lengthy. It was also apparent that presenting the computed values graphically or in a tabulated form can become bulky if a fairly broad range is to be covered. Hence, in order to facilitate the computations, an attempt will be made to approximate their relationships by some simple mathematical expressions. With these expressions, it is possible to obtain values for the center surface displacements without using long computational procedures.

To achieve this aim, two approaches are presented in the following sections.

Approach 1. In the study of the vertical motion of a circular "plate" resting on *elastic* ground, Reissner and Sung[40] tried to express the center displacement in terms of the polynomials of a_0, the dimensionless frequency ratio. That is

$$U_z(0,0) = f_1 + if_2 \qquad (92)$$

where

$$f_1 = c_{10} + c_{12}a_0^2 + c_{14}a_0^4, \tag{93a}$$

$$f_2 = c_{21}a_0 + c_{23}a_0^3 + c_{25}a_0^5, \tag{93b}$$

c_{10} to c_{25} are coefficients of the polynomial and their values depend upon the load distribution on the "plate" and the Poisson's ratio of the supporting medium. The coefficients are listed in Table IV.

Table IV. Coefficients of functions f_1 and f_2. (From Sung.[9])

ν	c	*Uniform pressure*	*Parabolic pressure*	*Rigid base*
1/4	c_{10}	–0.23873	–0.31831	–0.18750
	c_{12}	.05968	.04775	.07031
	c_{14}	– .00416	– .00238	– .00613
	c_{21}	.14859	.14859	.14859
	c_{23}	– .01776	– .01184	– .02368
	c_{25}	.00081	.00041	.00129
1/3	c_{10}	– .21221	– .28294	– .16667
	c_{12}	.05158	.04126	.06076
	c_{14}	– .00345	– .00197	– .00509
	c_{21}	.13063	.13063	.13063
	c_{23}	– .01504	– .01002	– .02005
	c_{25}	.00066	.00033	.00105
1/2	c_{10}	– .15916	– .21221	– .12500
	c_{12}	.03979	.03183	.04688
	c_{14}	– .00243	– .00139	– .00358
	c_{21}	.10455	.10455	.10455
	c_{23}	– .01104	– .00756	– .01472
	c_{25}	.00044	.00022	.00072

For a viscoelastic foundation, there should be a damping effect resulting from the dissipative properties of the medium. Hence, the first step of approximation is to consider the influence of $\tan \theta_2/2$ and replace f_1 and f_2 in eq 92 by their counterparts g_1 and g_2, which are defined as

$$g_1 = (g_1' + g_1'')\left(1 - \tan^2\frac{\theta_2}{2}\right) + 2(g_2' - g_2'')\tan\frac{\theta_2}{2} \tag{94a}$$

$$g_2 = (g_2' - g_2'')\left(1 - \tan^2\frac{\theta_2}{2}\right) - 2(g_1' + g_1'')\tan\frac{\theta_2}{2} \tag{94b}$$

and

$$g_1' = c_{10} + c_{12}a_0^2\left(1 - \tan^2\frac{\theta_2}{2}\right) + c_{14}a_0^4\left(1 - 6\tan^2\frac{\theta_2}{2}\right) \tag{95a}$$

$$g_1'' = (c_{21}a_0 + 3c_{23}a_0^3 + 5c_{25}a_0^5)\tan\frac{\theta_2}{2} \tag{95b}$$

$$g_2' = c_{21}a_0 + c_{23}a_0^3\left(1 - 3\tan^2\frac{\theta_2}{2}\right) + c_{25}a_0^5\left(1 - 10\tan^2\frac{\theta_2}{2}\right) \tag{96a}$$

$$g_2'' = 2(c_{12}a_0^2 + 2c_{14}a_0^4)\tan\frac{\theta_2}{2}. \tag{96b}$$

Thus, using the corresponding coefficients from Table IV, center displacements of a circular "plate" under the three types of loading conditions can be computed which include the effect of the damping property of the medium.

For the purpose of comparison, the values computed from the approximate expressions are checked against the integral solutions in the range of a_0 from 0.25 to 1.5 (with increment = 0.25) and tan $\theta_2/2$ from 0 to 0.1 (with increment = 0.02). Within this specified range, the difference in displacement amplitudes is generally within 3% with values from the approximate expressions usually larger. Only in some special situations, i.e. when both frequency and damping are high and for the Rigid Plate (approximation) loading condition, the differences are in the neighborhood of 4%. The difference for values of g_1 and g_2 are, however, considerably higher; from a few percent to as high as 20%. Since the large difference occurs mostly for small values of g_1 (or g_2), values of displacement amplitude are not really affected.

It appears, therefore, that results of this approach can be used to compute the center displacements of a circular source with good accuracy. However, a different approach may be needed for approximating the functions g_1 and g_2 if their values are of direct concern.

Approach 2. To include the damping effect from both tan $\theta_1/2$ and tan $\theta_2/2$, we introduce two functions ϕ_1 and ψ_1, each as a function of only one of the two damping constants. We further assume that g_1 may be represented by the product of ϕ_1 and ψ_1, i.e.

$$g_1\left(\nu, a_0, \tan\frac{\theta_1}{2}, \tan\frac{\theta_2}{2}\right) = \phi_1\left(\nu, a_0, \tan\frac{\theta_2}{2}\right)\psi_1\left(\nu, a_0, \tan\frac{\theta_1}{2}\right). \tag{97}$$

In this relationship, ϕ_1 and ψ_1 can be shown to take the form

$$\phi_1\left(\nu, a_0, \tan\frac{\theta_2}{2}\right) = \frac{f_1(\nu, a_0)}{1 + AA\tan(\theta_2/2)} \tag{98a}$$

$$\psi_1\left(\nu, a_0, \tan\frac{\theta_1}{2}\right) = 1 - CC(0.5 - \nu)\tan\frac{\theta_1}{2} \tag{98b}$$

where $f_1(\nu, a_0)$ is defined by eq 93a and AA and CC are coefficients with their values depending upon both ν and a_0.

To represent g_2, a similar approach may be employed. Let ϕ_2 and ψ_2 be the other two functions. Then we have

$$g_2\left(\nu, a_0, \tan\frac{\theta_1}{2}, \tan\frac{\theta_2}{2}\right) = \phi_2\left(\nu, a_0, \tan\frac{\theta_2}{2}\right)\psi_2\left(\nu, a_0, \tan\frac{\theta_1}{2}\right) \tag{99}$$

and

$$\phi_2\left(\nu, a_0, \tan\frac{\theta_1}{2}\right) = \frac{f_2(\nu, a_0)}{1 - BB\tan(\theta_1/2)} \tag{100a}$$

$$\psi_2\left(\nu, a_0, \tan\frac{\theta_1}{2}\right) = 1 + DD(0.5 - \nu)\tan\frac{\theta_1}{2} \tag{100b}$$

where $f_2(\nu, a_0)$ is defined by eq 93b and BB and DD are coefficients similar to AA and CC.

Values of AA, BB, CC, and DD are shown in Figures 15-17 for the three loading conditions. In each case they are plotted against a_0 for the three Poisson's ratios $\nu = 0.25$, 0.33, and 0.5.

Using these coefficients, the approximated values of g_1 and g_2 and also the complex amplitude at the circular center can be computed. Their values are again compared with the integral solution in the range of a_0 from 0.25 to 1.5, $\tan\theta_1/2$ from 0 to 0.15 and $\tan\theta_2/2$ from 0 to 0.1. In this range, the differences in computed amplitude are generally less than 1%, except at $a_0 = 0.25$ and $\tan\theta_1/2 = \tan\theta_2/2 = 0.1$. At these particular values of frequency and damping coefficients, the values from the approximate solution for the three loading conditions are off by 1½% - 3%. Values for g_1 and g_2 in this approach improve considerably. Their differences with the integral solutions are, in general, less than 2%.

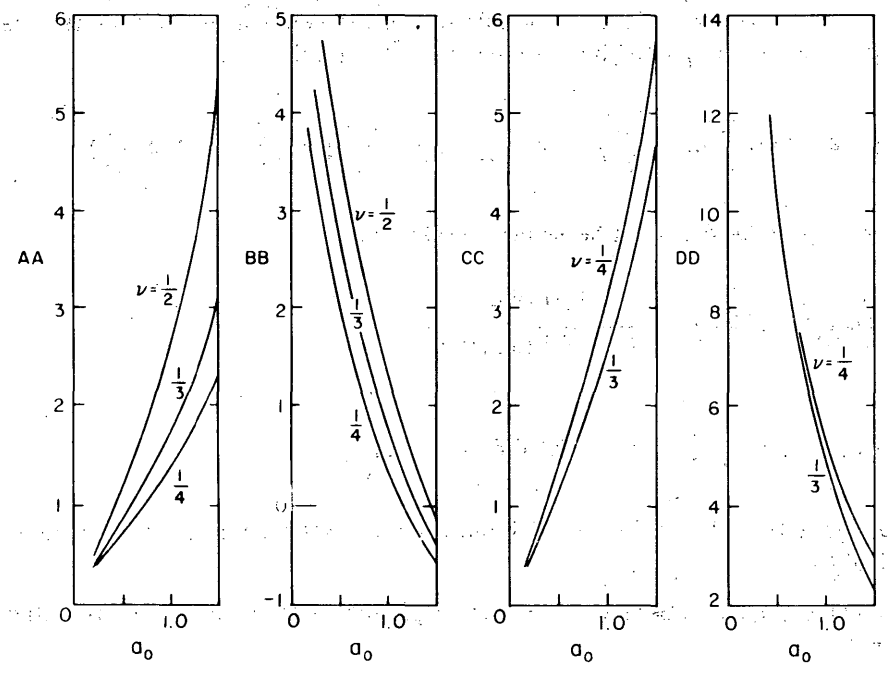

Figure 15. AA, BB, CC and DD vs a_0, uniform pressure source.

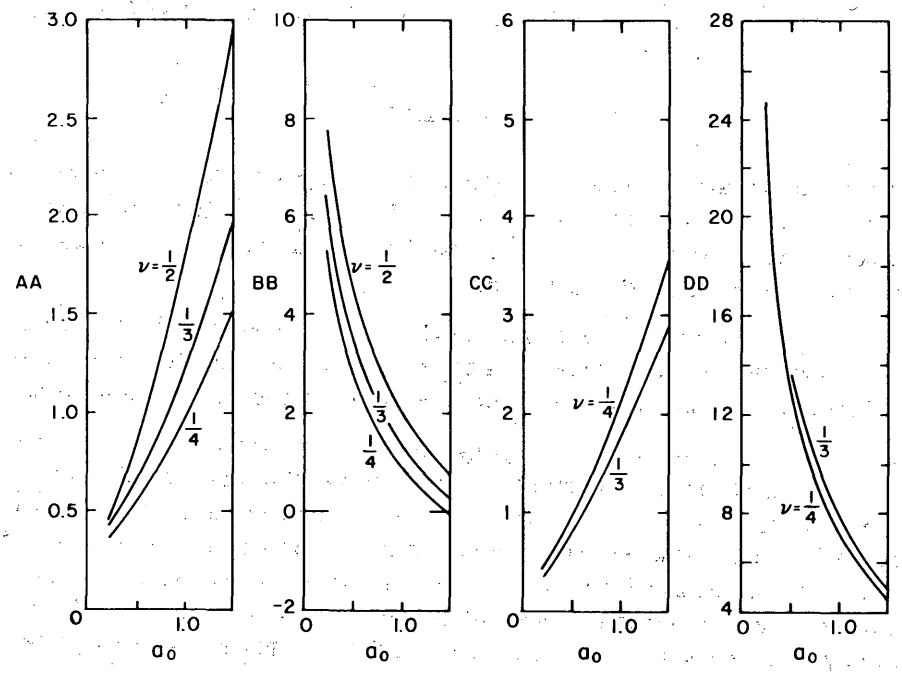

Figure 16. AA, BB, CC and DD vs a_0, parabolic pressure source.

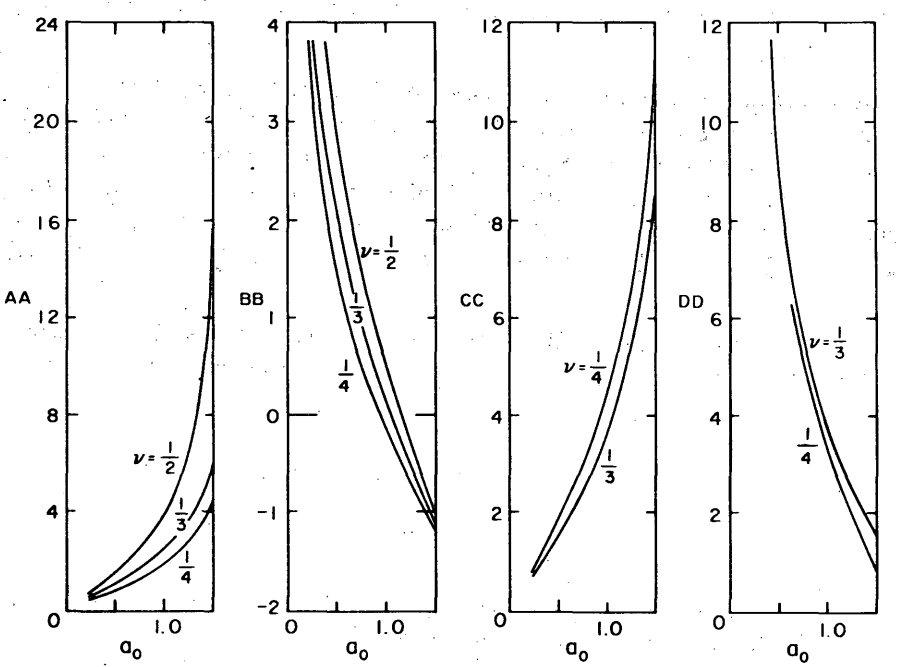

Figure 17. AA, BB, CC and DD vs a_0, rigid plate approximation.

CONCLUSION

Investigations of surface displacements with assumed types of pressure sources have indicated that simplified closed form solutions may be obtained for far field surface vibrations. In these areas, the effect of surface (Rayleigh) waves predominates and, therefore, material constants may be determined from surface vibration measurements.

Amplitudes of the displacement functions are shown to be related to the characteristics of the input source. Hence, unless these characteristics are known, determination of the ground properties through use of amplitude measurements at a *single* location will involve some uncertainty.

In addition to the terms affected by the properties of the source as mentioned, there is a common factor in all displacement functions regardless of the source. This factor indicates that displacement amplitudes vary inversely with the square root of the distance from the source and also decrease exponentially with a damping factor related to the damping properties of the medium. Therefore, if we apply the "Amplitude Ratio" technique of using surface measurements from *two* locations, the ground properties may be determined *without* knowing the characteristics of the source. In view of the uncertainty of the pressure distribution beneath the base plate of a testing vibrator, this technique may be desirable.

A study has also been made of the vertical displacements at the center of three assumed pressure loadings, namely uniform, parabolic, and rigid plate approximation. It was found that the complex displacement amplitudes may be expressed in terms of two real functions, g_1 and g_2, of their real and imaginary parts, respectively. In this form it is then possible to express these two functions directly in terms of the material properties of the supporting medium and the frequency of the applied load.

In order to facilitate computations, attempts have been made to approximate the above relationships by simple mathematical expressions. Two approaches have been employed. Both can provide fairly accurate values for the displacement amplitudes. Error in Approach 1 is found to be less than 3%, and that of Approach 2,1%. However, for calculating g_1 and g_2 (or the "mechanical resistance" and "mechanical reactance"), good accuracy can only be achieved by using the equations of Approach 2. The difference with the corresponding values from integral solutions is, in general, less than 2%.

The advantage of these approximations lies mainly in the fact that they replace a complicated numerical procedure but require only a small fraction of its computation time.

LITERATURE CITED

1. Department of Army, Office of Chief of Engineers (1967) Foundations subject to vibratory loads. Engineering and Design, EM 1110-345-310.

2. Hsieh, T.K. (1962) *Proceedings, Institution of Civil Engineers*, 22, 211.

3. Lamb, H. (1904) *Philosophical Transactions Royal Society of London* A, 203, 1-42.

4. Lee, T.M. (1963) Method of determining dynamic properties of viscoelastic solids employing forced vibration. *Journal of Applied Physics*, vol. 34, no. 5, p. 1524-1529. Also U.S. Army Cold Regions Research and Engineering Laboratory (USA CRREL) Research Report 122.

LITERATURE CITED (Cont'd)

5. Lee, T.M. (1963) Vibration of sphere for determining the dilatational constants of viscoelastic materials. *Journal of Applied Physics*, vol. 34, no. 8, p. 2150-2153.

6. _____ (1967) *Proceedings, International Symposium on Wave Propagation and Dynamic Properties of Earth Materials*, p. 123-138.

7. Quinlan, P.M. (1953) ASTM STP 156, Symposium on Dynamic Testing of Soils, 35, 3-34.

8. Reissner, E. (1936) Ingenieur-Archiv, 7, part 6, 381.

9. Sneddon, I.N. (1951) *Fourier transforms*. New York: McGraw-Hill.

10. Sung, T.Y. (1953) ASTM STP 156 Symposium on Dynamic Testing of Soils, 35, 35-63.

DOCUMENT CONTROL DATA - R & D

(Security classification of title, body of abstract and indexing annotation must be entered when the overall report is classified)

1. ORIGINATING ACTIVITY (Corporate author)
U.S. Army Cold Regions Research and Engineering Laboratory
Hanover, New Hampshire 03755

2a. REPORT SECURITY CLASSIFICATION
Unclassified

2b. GROUP

3. REPORT TITLE

VIBRATORY SURFACE LOADINGS ON A VISCOELASTIC HALF-SPACE

4. DESCRIPTIVE NOTES (Type of report and inclusive dates)

5. AUTHOR(S) (First name, middle initial, last name)
T.M. Lee

6. REPORT DATE
September 1970

7a. TOTAL NO. OF PAGES
36

7b. NO. OF REFS
10

8a. CONTRACT OR GRANT NO.

b. PROJECT NO.

c. DA Task 1T025001A130-01

d.

9a. ORIGINATOR'S REPORT NUMBER(S)
Research Report 286

9b. OTHER REPORT NO(S) (Any other numbers that may be assigned this report)

10. DISTRIBUTION STATEMENT
This document has been approved for public release and sale; its distribution is unlimited.

11. SUPPLEMENTARY NOTES

12. SPONSORING MILITARY ACTIVITY
U.S. Army Cold Regions Research and Engineering Laboratory
Hanover, New Hampshire 03755

13. ABSTRACT
Wave propagation generated by vibratory load on a homogeneous, isotropic, linear viscoelastic half-space is studied. The effect of a single concentrated force and a group of forces applied over a circular area has been examined and solutions of the displacement functions are presented. In the case of the group forces, the three types of force distribution used by Reissner and Sung were employed. At a great distance (far field) from the applied load, surface displacements are reduced to closed form expressions. A field method based on these results is recommended for determining the complex modulus and the damping property of a viscoelastic material. For areas near the source (near field), numerical procedures were employed to evaluate the integral solution. To facilitate the application, two simplified versions are provided for calculating the center displacement under the load. They both provide good approximation to the integral solution and, most important of all, they speed up the computation enormously.

14. KEYWORDS

Loads (forces)
Soil dynamics
Vibration
Vibration tests
Viscoelasticity
Wave propagation

DD FORM 1 NOV 68 1473 REPLACES DD FORM 1473, 1 JAN 64, WHICH IS OBSOLETE FOR ARMY USE.